

Alma Mater Studiorum Università di Bologna
Archivio istituzionale della ricerca

Preparation and assessment of the potential energy savings of thermochromic and cool coatings considering inter-building effects

This is the final peer-reviewed author's accepted manuscript (postprint) of the following publication:

Published Version:

Preparation and assessment of the potential energy savings of thermochromic and cool coatings considering inter-building effects / Berardi U.; Garai M.; Morselli T.. - In: SOLAR ENERGY. - ISSN 0038-092X. - STAMPA. - 209:(2020), pp. 493-504. [10.1016/j.solener.2020.09.015]

Availability:

This version is available at: <https://hdl.handle.net/11585/772828> since: 2022-12-23

Published:

DOI: <http://doi.org/10.1016/j.solener.2020.09.015>

Terms of use:

Some rights reserved. The terms and conditions for the reuse of this version of the manuscript are specified in the publishing policy. For all terms of use and more information see the publisher's website.

This item was downloaded from IRIS Università di Bologna (<https://cris.unibo.it/>).
When citing, please refer to the published version.

(Article begins on next page)

This is the final peer-reviewed accepted manuscript of:

Umberto Berardi, Massimo Garai, Thomas Morselli

Preparation and assessment of the potential energy savings of thermochromic and cool coatings considering inter-building effects,

In:

Solar Energy, Volume 209, 2020, p. 493-504

The final published version is available at:

<https://doi.org/10.1016/j.solener.2020.09.015>

Rights / License:

The terms and conditions for the reuse of this version of the manuscript are specified in the publishing policy. For all terms of use and more information see the publisher's website.

Preparation and assessment of the potential energy savings of thermochromic and cool coatings considering inter-building effects

Abstract

Cool coatings show high solar reflectance and have been proposed to decrease the building energy demand by reducing solar heat gains. However, cool coatings may have a negative effect during cold seasons when solar gains would be beneficial. Thermochromic coatings, thanks to their ability to change their solar reflectance at different temperatures, have been proposed to reduce the heating penalties during colder seasons of traditional cool coatings. In this work, four different thermochromic pigments have been used to create façade paints. The solar reflectance and thermal emissivity of these paints have been evaluated experimentally. A significant change of 0.37 in the reflectance of the four paints was registered in the visible range. These products are hence compared with common cool coatings available on the market. In order to evaluate the potential energy savings of thermochromic paints, an office building in downtown Toronto (Ontario, Canada) and the surrounding area have been modeled in Energy Plus. Different scenarios have been simulated and compared among conventional, cool, and thermochromic coatings applied on the roof or on the building facades. The study also evaluates the different new coatings under several climate change scenarios. Overall results show that for the context of analysis, thermochromic paints can provide an 8.9% decrease in the cooling demand, while limiting the winter penalties to 1.7%, compared to the heating penalties of 2.6% resulted using cool coating. Despite the limited heating penalties, the annual energy demand for all the simulated scenarios is comparable. Similar results were also obtained when the inter-building effects were taken into account in the analyzed context. Finally, thermochromic paints proved to be more beneficial considering future climate conditions as Canada is projected to show significantly higher cooling energy demands.

Keywords: Urban heat island, cool materials, thermochromic paint, solar reflectance, inter-building effects.

31 **1. Introduction**

32 Global temperatures have been growing steadily during the last three decades due to the
33 increasing emissions in the atmosphere of greenhouse gasses produced by human activities
34 (Ritchie & Roser, 2017). Meanwhile, the current climate change mitigation strategies are not
35 keeping up with the targets set in the Paris Agreement (Paris Agreement, 2016). In particular, as
36 buildings account for 36% of global final energy use and 39% of energy-related carbon dioxide
37 emissions (UN Environment, 2017), they are often indicated as the sector urgently needing
38 solutions for a low-carbon future.

39 Improving the performance of the building envelope is a trending theme of research. The
40 development of new building materials promises to represent a significant opportunity to reduce
41 building energy demand and emissions (Ascione, 2017). Among new materials, reflective
42 coatings represent a cost-effective and environmentally friendly alternative for building
43 finishing. Characterized by a high solar reflectivity and thermal emissivity, cool coatings can
44 reduce surface temperature leading to a reduction of the cooling demand (Synnefa et al., 2007;
45 Synnefa & Santamouris, 2013; Hosseini & Akbari, 2014; Jandaghian and Berardi, 2020). Cool
46 materials have demonstrated to bring substantial benefits, especially in hot climates. However,
47 their static behavior becomes a limit in those climates with cold seasons and hot summer, where
48 a dynamic response of the building envelope becomes critical (Wang et al., 2016).

49 As cool materials continuously reflect solar heat gains, these have may counterproductive effects
50 during the cold season. Consequently, the demand for dynamic or responsive coatings, that could
51 change their behavior according to environmental conditions, has emerged. In this context,
52 thermochromic pigments have received increasing attention thanks to their variable thermo-
53 optical properties that reversibly change accordingly to the temperature. This transformation
54 allows thermochromic pigments to display a lighter and more reflective color during the hot
55 periods of the year, and an absorbing behavior when the outdoor temperature decreases together
56 with their solar reflectance (Karlessi & Santamouris, 2013).

57 Thermochromic coatings are already used in a variety of fields from packaging to clothing and
58 medical products. A typical application in the building field of the thermochromic behavior is
59 represented by thermochromic windows (Zheng et al., 2015; Yuanyuan et al., 2018). In these
60 systems, the phase transition associated with a relevant change in the optical properties in the
61 near-infrared range makes the thermochromic windows able to manage the solar heat gains
62 dynamically. Similarly, thermochromic coatings could be adopted to control the heat gain of the
63 opaque portion of the envelope, although a few studies on thermochromic coatings exist so far.

64 This study aims to compare both experimentally and numerically cool and thermochromic
65 coatings; for this, the energy consumption variations of a building in a continental climate
66 resulting from the application of different coatings are assessed. The research includes a
67 laboratory characterization of thermo-optical properties including the solar reflectance, the
68 thermal emissivity, and the solar reflectance index (SRI) of new cool and thermochromic paints.
69 The following building-scale energy demand analysis is also conducted considering the inter-
70 building effects. A final analysis focuses on the implication of climate change and the
71 effectiveness of both cool and thermochromic paints over building energy demands under future
72 climate scenarios.

73

74 **2. Literature review**

75 Exterior coatings influence the thermal behavior of the building envelope according to two
76 parameters, the solar reflectance and the infrared emittance. While conventional dark-colored
77 coatings usually have a low solar reflectance, cool coatings have a high solar reflectance and
78 thermal emissivity. A coating with high solar reflectance decreases the absorption of incoming
79 electromagnetic radiations. On the other hand, high thermal emittance allows a rapid dispersion
80 of the absorbed heat, and a faster surface temperature decrease (Santamouris et al., 2011). The
81 adoption of highly reflectivity materials is a promising mitigation technique for the urban heat
82 island phenomenon since lower surface temperatures lead to less heat transfer to the ambient air
83 (Synnefa et al., 2008, Wang et al., 2016). Haberl and Cho (2004) reported that cooling energy
84 savings from the application of cool materials on residential and commercial buildings vary from
85 2% to 44%, while the peak cooling energy savings are between 3% and 35%, depending on
86 building characteristics. Moreover, the reduced heat transfer leads to a lower temperature in the
87 indoor environment and an increase in thermal comfort. In 2007, a study compared the behavior
88 of a single-story building with a flat roof in 27 cities, and found that the adoption of a highly
89 reflective roof with a solar reflectance of 0.85 caused a reduction of the maximum temperature
90 between 1.2– 3.7°C and of the discomfort hours between 9% and 100% (Synnefa et al., 2007).
91 However, the benefits of cool materials are higher when cool coatings are adopted in poorly
92 insulated buildings (Fabiani et al., 2020). Together with lower surface temperatures, a higher
93 solar reflectance of the roof coatings increases the lifetime of the roof as it would reduce the
94 thermal fatigue and chemical degradation mechanisms (Pisello, 2017).
95 The effectiveness of cool coatings depends on the climatic conditions, as high albedo coatings
96 are more effective in hot climates and at lower latitudes, where the building cooling load
97 significantly exceeds the heating one. In fact, the reflection of the incoming radiation during the

98 heating periods and reduces free heat gain increases, even if the winter penalties are limited by
99 lower sun angles, cloudier days, shorter daytime, and the chance of snow accumulation (Hosseini
100 et al., 2014). In recent years, studies have investigated new coatings capable of adapting to
101 different seasonal conditions and needs. Among the various solutions, thermochromic materials
102 have gained significant attention. These products exhibit a relevant color change, accompanied
103 by variations of their optical and thermal properties when exposed to a specific temperature. The
104 temperature range at which the transformation occurs is called transition or switching
105 temperature (Garshasbi & Santamouris, 2019). Temperature-sensitive optical properties allow to
106 respond to different external environment changes: when thermochromic materials substitute a
107 standard building coating, the new finishing could behave like a “conventional” cool roof during
108 hot periods, while transitioning to a darker color during the cold seasons when they would
109 absorb more solar radiation.

110 The current state of the art of thermochromic materials has been summarized by Garshasbi and
111 Santamouris (2019) with specific attention to the possible application in the building sector.
112 Currently, laboratory analysis has been conducted mainly on Leuco dyes (Zheng et al., 2015;
113 Fabiani et al., 2019; Zhang & Zhai, 2019), which have a temperature transition consistent with
114 the building sector and a low cost of production. Leuco dye thermochromic mechanism is a
115 result of the interaction between three elements: color former, color developer, and co-solvent.

116 Measurements of the solar reflectance spectra of various thermochromic coatings have been
117 carried out, and the results proved a significant change in the visible region, while a negligible
118 effect has been recorded in the near-infrared one. Fabiani et al. (2019) used black
119 microencapsulated leuco-based thermochromic pigments to produce a solvent-based coating with
120 a solar reflective coefficient switch between 0.35 and 0.55 for the colored and non-colored
121 phases, respectively. The optical properties of thermochromic coating are influenced by the
122 concentration and size of the thermochromic pigment and by the concentration of the TiO₂
123 molecules (Zhang & Zhai, 2019). The introduction of TiO₂ particles in thermochromic paint
124 increases the solar reflectance and the difference between the two phases (Zhang & Zhai, 2019;
125 Xiong & Jianying, 2019).

126 Currently, the main downside of cool and thermochromic coatings is their aging (Morini et al.,
127 2018). The primary degradation mechanism that reduces the thermochromic transformation is
128 the UV radiation (Karlessi et al., 2009). Recently, Karlessi and Santamouris (2013) proved that a
129 combination of UV and optical filters could limit the solar reflectance variation of the paint
130 during both phases.

131 The potential energy saving of thermochromic coatings when applied to building envelopes is a
132 relatively new field of investigation. Just a few studies have investigated the benefits of this
133 technology by modeling prototype buildings using energy modeling (Zheng et al., 2015; Jianying
134 & Xiong, 2019; Park & Krarti, 2016). Different procedures have been adopted to simulate the
135 dynamic behavior of thermochromic paints. Park and Krarti (2016) used two reflectivity values
136 for two periods: a solar reflectivity of 0.55 during the cooling period and a reduced 0.30 value
137 during the heating period. Similarly, Zheng et al. (2015) performed an analysis on a small box;
138 the reflectance of the coating was monthly selected based on the average air temperature, if the
139 temperature was higher than 25°C, the coating was assumed to be in its colorless phase for the
140 entire month. Jianying and Xiong (2019) performed a more precise analysis: the dynamic optical
141 properties of thermochromic paints were modeled using the energy management system (EMS)
142 in EnergyPlus, so it changed accordingly to the surface temperature. Jianying and Xiong (2019)
143 investigated the energy consumption in seven cities representing the different U.S. climate zones
144 confirming that thermochromic paints are especially effective in regions with high cooling and
145 heating demands, like Chicago or Portland. Compared to a conventional roof, cool coatings and
146 thermochromic coatings mixed with TiO₂ reduced the annual cooling electricity demand by 8.9–
147 23.3 kWh/m² and 2.9–15.1 kWh/m² respectively, which corresponded to a decrease between the
148 17.2 to 54.5% and 11.1 to 39.4% of the cooling demand. However, when the heating loads were
149 taken into account, the thermochromic coatings guaranteed the best performance.

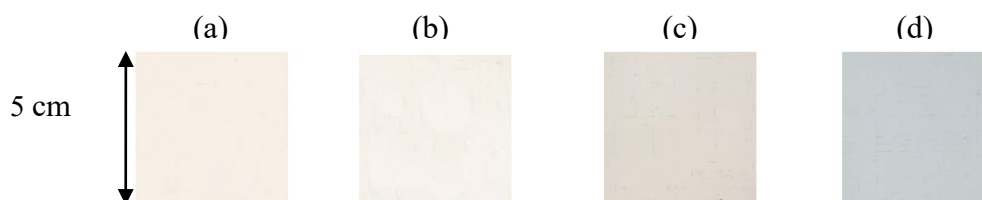
150

151 **3. Methodology**

152 **3.1 Laboratory characterization**

153 **3.1.1 Sample development**

154 Four cool coatings, developed by two companies Kool Seal and Lanco, were selected and
155 evaluated. The coatings were applied to brick squared samples (5x5 cm) in two layers, as
156 represented in Fig. 1.



157 **Figure 1.** Cool paint samples considered in this study: (a) Kool Seal Premium, (b) Kool Seal RV, (c) ultra
158 siliconizer, and (d) urethanizer.

159

160 To design a thermochromic paint, four microencapsulated leuco dyes thermochromic in powder
 161 form were purchased from different companies (Table 1). The paints were created using two
 162 components: an acrylic water-based base paint, characterized by a high concentration of TiO₂
 163 molecules (14%), and the thermochromic powder mixed in different concentrations to assess
 164 different levels of the thermochromic effect. Three types of coating have been prepared for each
 165 thermochromic product, using three concentrations of the powder: 5%, 10%, and 15%. Different
 166 amount of thermochromic particles have been tested to evaluate their impact on the solar
 167 reflectance value during the colored and non-colored phase. The components were stirred
 168 manually to avoid the damaging of the microcapsule. Two hands of the thermochromic paints
 169 have been applied to each brick as done for the cool paints.

170

171

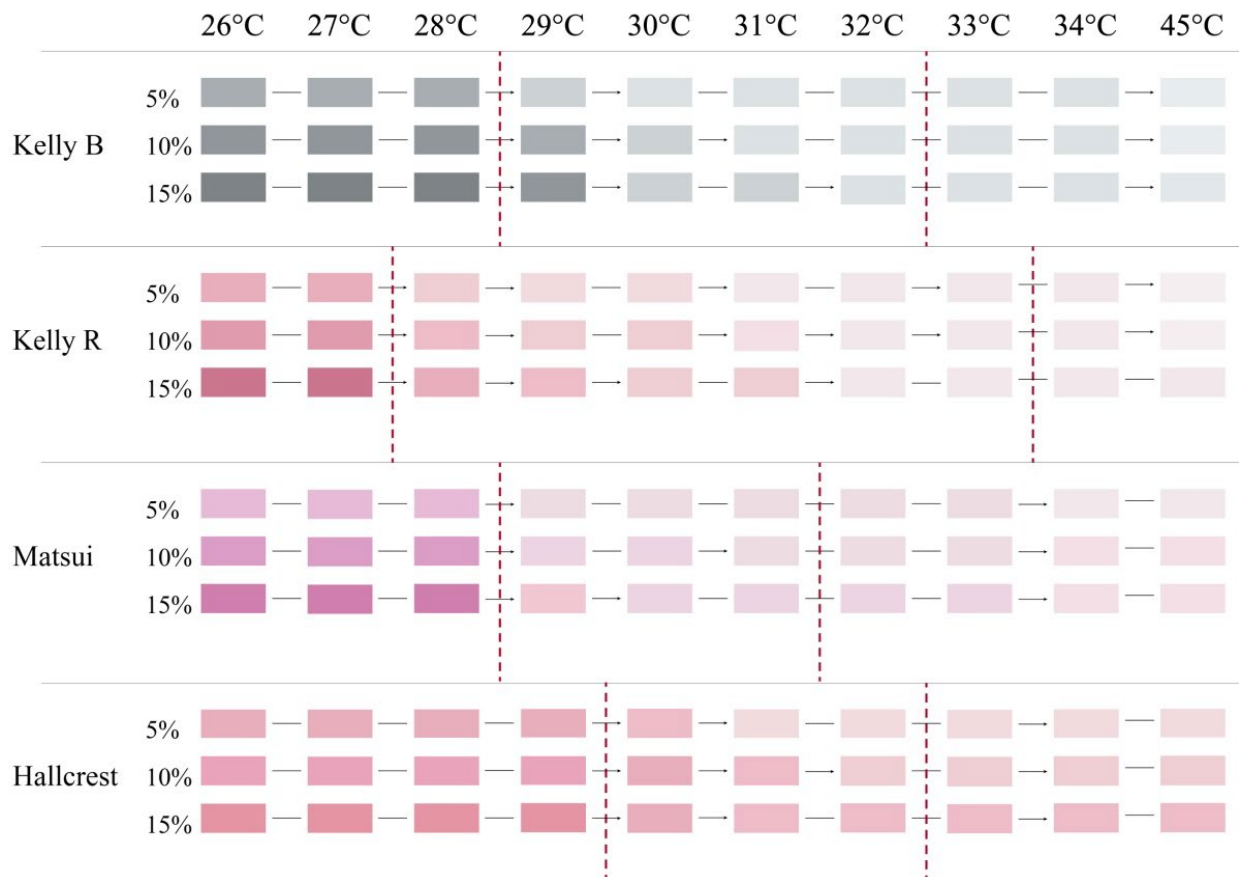
Table 1. Characteristics of the thermochromic considered in this study.

Product	Company	Color	Transition temperature	Particle Size
Thermochromic Red RT-31BF	Kelly Chemical Corporation	red	31°C	10 ± 2 μm
Thermochromic Black LT-31BF	Kelly Chemical Corporation	black	31°C	10 μm (max)
Chromicolor® MS Powder LF Grade	Matsui Shikiso Chemical Co.	magenta	25°C	2-4 μm (average)
Thermochromic Powder BPA Free_Red 31	LCR Hallcrest	red	31°C	<6 μm (97%)

172

173 Each thermochromic paint proved to have different behaviors. All samples were simultaneously
 174 exposed to the same environmental condition inside a climatic chamber which was programmed
 175 to raise the temperature from 26°C to 34°C at 1°C temperature steps. Each temperature set-point
 176 was maintained for 30 minutes after which a manual evaluation of the color change of the
 177 specimens was performed using a color palette. The color transformation resulted to be gradual
 178 for some products like Kelly Powder, while others, like Mastui, showed a more rapid
 179 transformation.

180 All the tested paints proved to be highly reactive to the transition temperature when heated. The
 181 percentage of thermochromic powder had no impact on the temperature and duration of the
 182 thermochromic transition. However, the higher percentages of thermochromic particles led to
 183 more saturated colors, as evident in Fig. 2.



184 **Figure 2.** Thermochromic transition temperature and transition range comparison. The red dotted lines
 185 identify the temperature thresholds at which the thermochemical transformation occurs.

186
 187 The measurements of the recovery time, e.g., the time required to return to the colored phase,
 188 proved that the inverse transition was slowed for all products. All samples were simultaneously
 189 exposed to the same lab conditions (air temperature of 23 °C and relative humidity of 20%), and
 190 the process was considered concluded when the color of the previously heated samples was the
 191 same as the reference ones already placed in the lab. The sample with the shortest recovery time
 192 (15 minutes) was the one developed with the black Kelly Powders; while the paint developed
 193 with the Hallcrest red powder required 40 minutes to recover fully.

194
 195 **3.1.2 Optical characterization**

196 Two thermo-optical properties were evaluated, the solar reflectance (ASTM E903-12) and the
 197 thermal emittance (ASTM E1933-14). The resulting values have been used as input data to
 198 calculate the solar reflectance index (SRI) in compliance with the (ASTM E1980-11).
 199 The total solar reflectance of the samples was tested using the Cary 5000 UV-Vis-NIR
 200 spectrophotometer coupled with an internal diffuse reflectance accessory (DRA) consisting of a
 201 110 mm diameter integrating sphere (DRAs). The instrument was calibrated using a

202 Polytetrafluoroethylene (PTFE) disk, provided by the Agilent Company. Once the spectral
203 reflectance was obtained, the solar reflectance was computed using the 100 selected ordinates
204 derived from Tables G173 of ASTM E903 (2012).

205 The visible reflectance was measured in a similar way by selecting all the ordinates from the
206 Tables G173 of ASTM E903 (2012) included between visible range boundaries. The solar
207 reflectance of the colored and colorless phase of the thermochromic paints was measured
208 separately. A hot plate was used to heat the coated bricks to 40 °C to make sure that the paints
209 would have remained uncolored throughout the entire measurement period. The surface
210 temperature was monitored using thermocouples. Similarly, to evaluate the solar reflectance of
211 the colored phase, the samples were cooled down to 15 °C.

212 To measure the thermal emissivity, the Haida Climatic Test Chamber HD E702 was used
213 together with a Fluke Ti450 PRO Infrared Camera. The tests were performed according to the
214 ASTM E1933 (2014) following the noncontact thermometer method. As a surface-modifying
215 material, a black tape characterized by an emissivity of 0.95 was attached to each sample. To
216 heat the paints uniformly, all the samples were placed inside the climatic test chamber at a
217 controlled temperature of 40 °C (10 °C higher than the transition temperature and 18-23 °C more
218 elevated than the ambient temperature) for approximately 25 minutes. The images were taken at
219 a distance of 50 cm in a controlled lab environment with an air temperature of 23 °C and a
220 relative humidity of 20%. The infrared images were processed using the SmartView 4.3 software
221 to calculate the actual thermal emissivity, following the methodology reported in other recent
222 studies (Soudian et al., 2020).

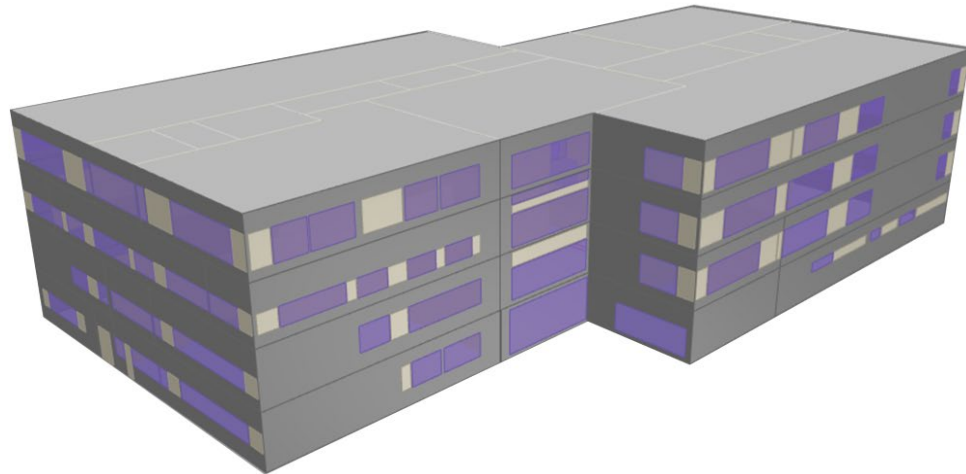
223

224 **3.2 Simulations**

225 **3.2.1 Case study**

226 The thermochromic coatings were also assessed on a case study building. For this scope, one
227 educational building located in downtown Toronto (Ontario, Canada) was selected. The
228 reasoning for this selection was the desire to assess thermochromic coatings in a continental
229 climate with high heating and cooling loads; moreover, the selection of an office building
230 allowed to consider better the impact that solar gains have on such a typology of buildings,
231 whose energy load is mainly influenced during daytime hours. Finally, the selection was done
232 for one building of the Ryerson University as this is currently in the process of being retrofitted
233 and there is interest in assessing the impact of the color of the finishing layers over the present
234 and future building energy demand.

235 The model was simulated using the CWEC 2016 weather file provided by Environment Canada.
 236 The building energy model was reconstructed from the architectural and mechanical drawings,
 237 kindly provided by Thom Partnership architectural firm. An ideal load air system object was
 238 designed to simulate a hypothetical HVAC system that provides an unlimited amount of air at a
 239 specific temperature when the set-points specified in the schedules were not met. The
 240 characteristics of the building energy model are reported in Table 2.



241 **Figure 3.** Energy model of the case study building designed with Honeybee.
 242

243 **Table 2.** Main building characteristics of the educational building of Ryerson University.

General parameter	value	Envelope	U-Value [W/m ² K]
building floor area / conditioned	6300 m ² / 6000 m ²	Roof	0.37
gross wall area / roof area	2900 m ² / 1800 m ²	exterior wall	1.18
window to wall ratio	23%	ground floor	0.63
N° of thermal zones	62	windows	3.95
N° of conditioned zones	54	spandrel panels	6.67

244
 245 **3.2.2 Energy demand analysis**
 246 The results obtained by the laboratory tests have been used as input data to simulate the potential
 247 energy savings that could be achieved if the thermochromic paints are applied on the envelope of
 248 the case-study building. The possible aging and shorter life expectancy of thermochromic
 249 pigment in the outdoor environment was neglected.
 250 Four types of analysis have been conducted, as summarized in Table 3. Out of the
 251 thermochromic paints created and tested, only the most performing sample was simulated. The
 252 paint produced with the Black LT-31BF Kelly powder with a 15% concentration proved to be

253 the one characterized by the largest solar reflectance difference between the two phases.
 254 Moreover, it is the paint with the lowest solar reflectance during its dark stage, leading to
 255 probable lower heating penalties.

256 Three different coatings have been compared: conventional low reflective paint, cool paint, and
 257 thermochromic paint. Four scenarios have been investigated: firstly, the current situation has
 258 been analyzed, where both horizontal and vertical surfaces have been coated with conventional
 259 low reflecting paint; afterward, the roof has been covered with cool and thermochromic paints;
 260 finally, the effects of thermochromic paints applied on the walls have been simulated.

261

262

Table 3. Type of analysis for the several investigated scenarios.

	Energy consumption	Parametric	Context	Climate change
Roof	1) Conventional		1) Conventional	1) Conventional
	2) Cool	TCM	2) Cool	2) Cool
	3) TCM lab paint		3) TCM lab paint	3) TCM lab paint
Façade	1) Conventional	-	1) Conventional	1) Conventional
	4) TCM lab paint		4) TCM lab paint	4) TCM lab paint

263

264 Thermochromic paints were simulated in Energy Plus using the Energy Management System
 265 (EMS) components. This allowed to change the value of the material properties during the
 266 simulations dynamically. The thermo-optical properties of the paints are reported in Table 4.

267

268

Table 4. Thermo-optical properties of the different coatings used as input for the simulation.

	Solar absorptance	Visible absorptance
Conventional	0.8	0.8
Cool	0.2	0.2
Thermochromic	0.4 for $T \leq 28^{\circ}\text{C}$	0.63 for $T \leq 28^{\circ}\text{C}$
	F(T) linear for $28^{\circ}\text{C} \leq T \leq 32^{\circ}\text{C}$	F(T) linear for $28^{\circ}\text{C} \leq T \leq 32^{\circ}\text{C}$
	0.2 for $T \geq 32^{\circ}\text{C}$	0.26 for $T \geq 32^{\circ}\text{C}$

269

270 3.2.3 Parametric analysis

271 A parametric investigation of the thermo-optical properties to optimize the performance of the
 272 thermochromic coatings was also performed. Two parameters were manipulated to investigate

273 the dynamic behavior of thermochromic coating: the visible absorptance that characterized both
274 phases, and the transition temperature.

275 The visible absorptance is the only thermo-optical parameter that changes accordingly to the
276 outdoor temperature, while no variation has been observed during the laboratory tests and in
277 previous studies (Zheng et al., 2015; Fabiani et al., 2019; Zhang & Zhai, 2019) in the near-
278 infrared and ultraviolet range of the solar spectrum. The total solar absorptance value has been
279 calculated considering the solar radiation distribution in the electromagnetic spectrum; more
280 precisely, the visible radiations (45%), the ultraviolet radiations (5%), and the near-infrared
281 radiations (Synnefa and Santamouris, 2013). To describe the dynamic behavior of the paint, a 0.3
282 visible absorptance variation has been considered, according to the results obtained in previous
283 studies and from the spectrophotometer analysis. Therefore, the visible solar absorptance of the
284 paint during the two different phases can be described as follows:

$$285 \quad VIS_{abs,Coloreless} = VIS_{abs,Colored} - 0.3 \quad (1)$$

286 The other parameters selected for this investigation is the transition temperature, while the
287 transition temperature range has been kept constant to a 4 °C.

$$288 \quad Solar\ Absorptance_{dark} < T_{trans} ; Solar\ Absorptance_{light} > T_{trans} + 4 \quad (2)$$

289 In total, 30 different thermochromic paints have been simulated on the roof of the building. The
290 number of different scenarios is the result of the combination of six different transition
291 temperatures ($T_{trans} = 15$ °C, 18 °C, 21 °C, 24 °C, 27 °C, and 30 °C) and five visible
292 absorptance values ($VIS_{abs,Colored} = 0.5, 0.6, 0.7, 0.8, \text{ and } 0.9$).

293

294 **3.2.4 Context analysis**

295 The introduction of the surrounding constructions around the case study building has been
296 evaluated. Since the incident solar radiation heavily influences the behavior of the
297 thermochromic paint, it is necessary to evaluate their performance if the context is introduced.
298 The floor plans of the surrounding buildings have been reconstructed using the available Open
299 Street Map data.

300

301 **3.2.5 Climate change impact**

302 To assess the impact of climate change on the heating and cooling demand of the case study
303 building and understanding the corresponding consequences on the studied paints, a cross-
304 comparison analysis was performed, and the four scenarios have been investigated using future
305 weather files. In this study, future weather files created by Berardi and Jafarpur (2020) using the
306 WeatherShift™ tools were adopted. The WeatherShift™ tools use the imposed offset method to

307 statistically downscale Global Climate Models for future weather file generation establishing a
 308 correlation between Global Climate Models and historical local weather data. The worst-case
 309 emission scenario (RCP8.5), which considers a rise of the emission throughout the 21st century,
 310 and the period of 2056–2075 projection timeframe have been used to create the future weather
 311 file.

312

313 4. Results

314 4.1 Laboratory characterization

315 The spectrophotometer measurements conducted on the four cool paints are illustrated in Fig. 4;
 316 each line has been obtained as an average of the two measurements carried out on the two
 317 sample sets. All the four coatings show a high total reflectance since the reflectance coefficient is
 318 relevant both in the visible and near-infrared range where the majority of the solar spectrum is
 319 concentrated. The sample with the lowest solar reflectance is the Lyanco Urethanizer. Table 5
 320 summarizes the solar and visible reflectance value measured. All products showed a thermal
 321 emissivity of approximately 0.9, meaning that the paint can emit the absorbed radiation quite
 322 easily in this specific portion of the spectrum.

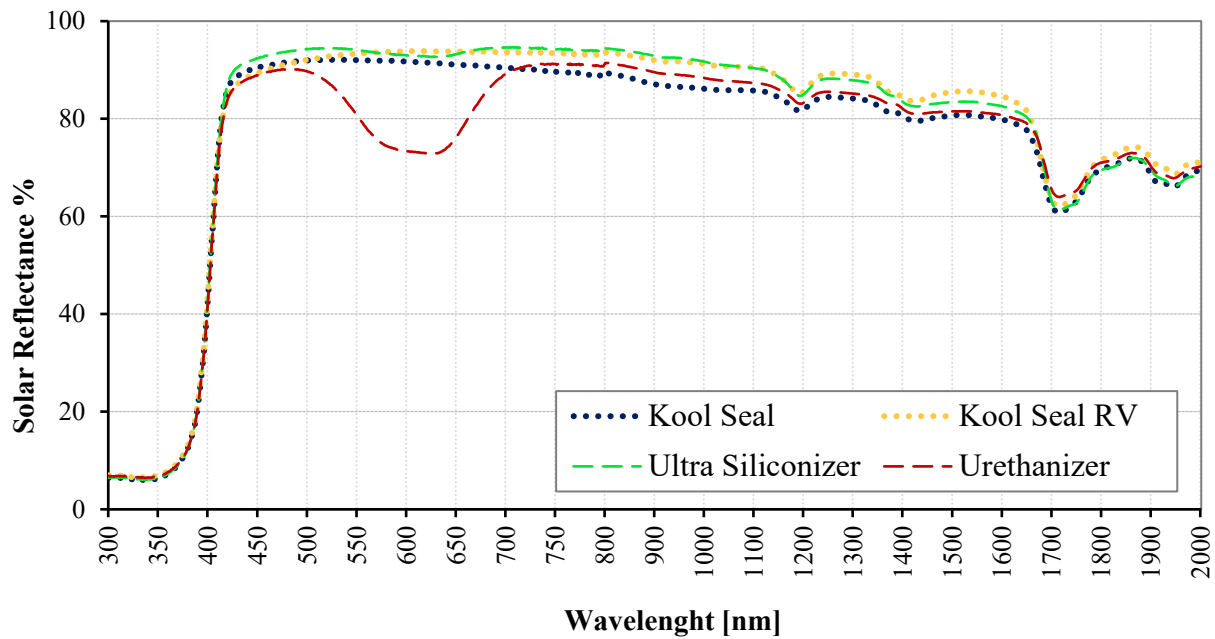
323 The thermal emissivity and the solar reflectance values, together with a convective coefficient
 324 assumed to be $12 \text{ W/m}^2\text{K}$ (i.e., a common wind condition), allow the calculation of the SRI
 325 values of the four products. Since all the tested paints have a similar thermal emittance, the most
 326 influential parameter is the solar reflectance. The Ultra Siliconizer has the highest solar
 327 reflectance index (110), followed by two Kool Seal products (Kool Seal RV 108 and Kool Seal
 328 105), while the lowest value was recorded for the Urethnizer paint (102). All the samples show
 329 an index higher than 100 since the solar reflectance of all the paints is larger than the white
 330 reference surface (0.8).

331

332

Table 5. Cool paint solar and visible reflectance results comparison.

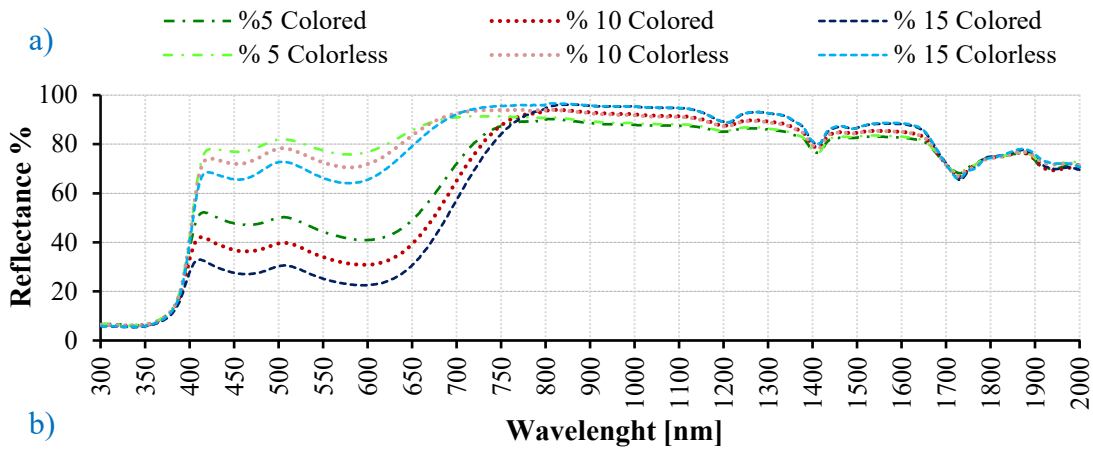
	Solar R%			Visible R%		
	Set A	Set B	<i>average</i>	Set A	Set B	<i>average</i>
Ultra Siliconizer	0.88	0.87	<i>0.87</i>	0.91	0.90	<i>0.91</i>
Urethanizer	0.84	0.80	<i>0.82</i>	0.83	0.81	<i>0.82</i>
Kool Seal	0.84	0.84	<i>0.84</i>	0.89	0.88	<i>0.88</i>
Kool Seal RV	0.88	0.83	<i>0.86</i>	0.91	0.87	<i>0.89</i>



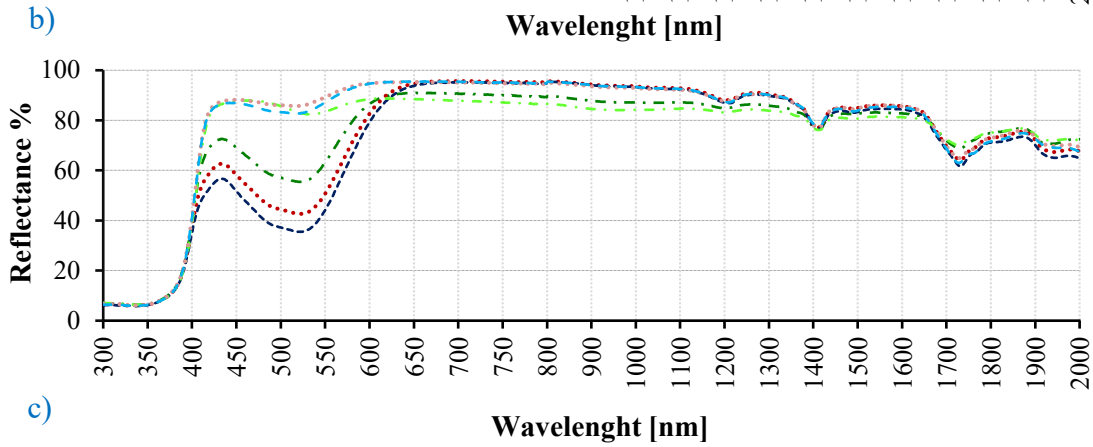
333
 334 **Figure 4.** Solar reflectance spectrum for the four cool paints considered in this study.
 335

336 Thermochromic paint proved to be highly reflective, too. However, the thermochromic
 337 transformation proved to affect the visible reflectance of the paint, modifying the total solar
 338 reflectance accordingly to the sample temperature. Small differences were observed in the NIR
 339 and UV regions: short wave radiations are absorbed by the samples, while the vast majority of
 340 the long wavelengths are reflected even when the samples are colored, as illustrated in Fig.5. The
 341 percentage of thermochromic particles influenced the color saturation and thus the reflectivity of
 342 the paint. A higher amount of particle inserted in the mix led to a lower visible reflectance,
 343 especially during the colored phase.

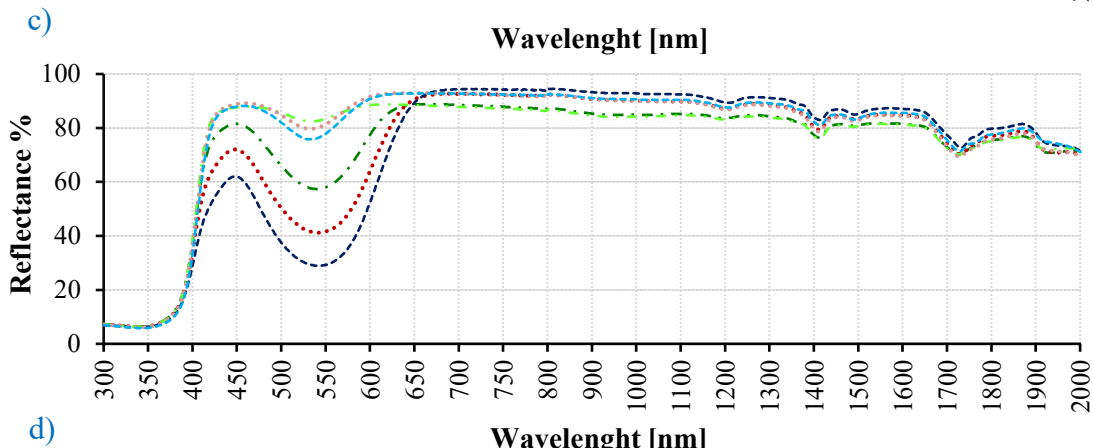
344 The paints Hallcrest and KEL_R have a similar trend, both characterized by a peak in the red
 345 region of the visible range (600 nm), the samples, in fact, have a similar color. The black
 346 specimens (KEL_B) have no specific peak; these samples achieve lower values of solar and
 347 visible reflectance since the black powder absorbed more radiation compared to red pigments.



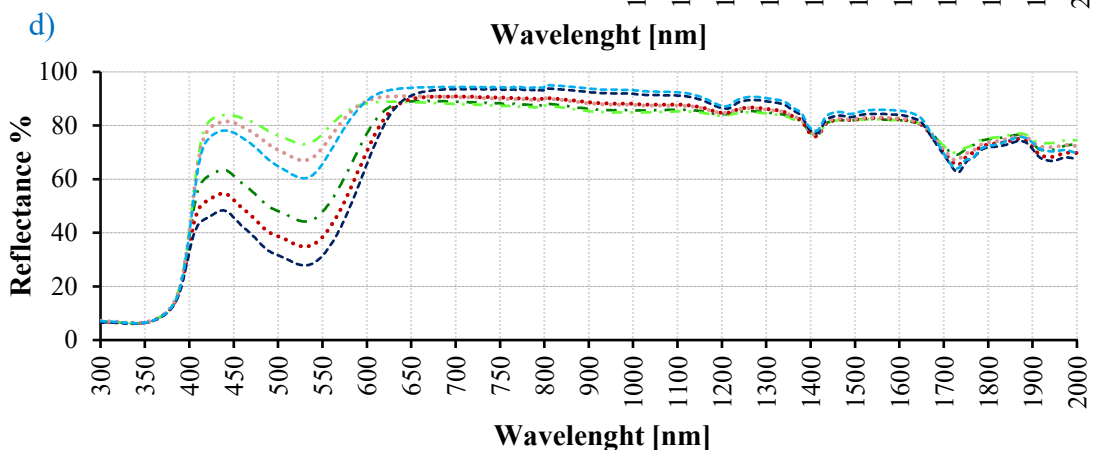
348



349



350



351

352 **Figure 5.** Thermochromic total solar reflectance spectrum for the four thermochromic coatings
 353 considered in this study: a) Kelly_B; b) Kelly_R; c) Matsui; and d) Hallcrest.

354

355 Among the developed samples, the paint produced using the highest concentration of the Kelly
 356 Black powder achieved the highest solar reflectance difference between the two phases (Table
 357 6). A visible reflectance variation of 0.37 has led to a change of the total solar reflectance of 0.2.
 358 All the samples reached a high level of reflectance during the colorless phase due to the high
 359 percentage (14%) of TiO₂ contained in the base solution.

360
 361 **Table 4.** Solar and visible reflectance of thermochromic samples, colored and colorless phase:
 362 comparison between the different percentages of thermochromic powder.

Product	Phase	TCM concentration	Solar R%	Visible R%	ΔR% Solar	ΔR% Visible
KELLY_B	Colored	5%	66	54	/	/
		10%	63	45	/	/
		15%	60	37	/	/
	Colorless	5%	81	80	+15	+26
		10%	81	78	+18	+33
		15%	80	74	+20	+37
KELLY_R	Colored	5%	78	75	/	/
		10%	77	71	/	/
		15%	75	67	/	/
	Colorless	5%	85	88	+7	+13
		10%	87	89	+9	+18
		15%	86	88	+11	+21
MATSUI	Colored	5%	77	75	/	/
		10%	75	68	/	/
		15%	72	62	/	/
	Colorless	5%	81	84	+5	+9
		10%	84	86	+9	+18
		15%	84	85	+12	+23
LCR	Colored	5%	73	68	/	/
		10%	72	64	/	/
		15%	71	61	/	/
	Colorless	5%	80	82	+5	+9
		10%	81	81	+9	+18
		15%	82	80	+12	+23

364 All the products have comparable thermal emittance values (0.9), and no significant differences
 365 have been registered between paints with different concentrations of thermochromic. All the
 366 solar reflectance indexes were mainly influenced by the variation of the solar reflectance value
 367 (Table 7). In the colorless phase, all the samples show a value higher than 100 since the solar
 368 reflectance of all the paints is larger than the reference surface. High values have been obtained
 369 even for the colorless phase of each sample. Even if these values are comparable to the one
 370 registered for the cool coating is essential to remind that there is a higher concentration of TiO₂
 371 particle in the thermochromic samples compared to the cool ones. Moreover, the values obtained
 372 by the thermochromic samples are representable of a basic and simple receipt, while the tested
 373 cool coatings are products entirely developed, with more components mixed.

374
 375 **Table 5.** SRI value of the thermochromic samples: evaluation of the impact of various percentage of the
 376 thermochromic in the coating.

SRI	5% colored	10% colored	15% colored	5% colorless	10% colorless	15% colorless
Kelly_B	81	77	73	101	102	100
Kelly_R	97	96	93	107	110	108
Matsui	96	93	89	101	106	106
Hallcrest	90	89	88	100	102	103

377
 378 **4.2 Simulation analysis**
 379 **4.2.1 Energy consumption analysis**
 380 Initially, the model has been tested without the implementation of an HVAC to understand the
 381 effect of the different paints on the indoor air temperature. This was necessary to evaluate the
 382 actual indoor temperature, avoiding the air condition system to bring the temperature to the
 383 prefixed set points. Two thermal zones have been studied: a zone located on the top floor of the
 384 building, at direct contact with the roof, and a zone located on the first floor of the building. Both
 385 spaces have the same orientation (northwest) and a comparable dimension and window to wall
 386 ratio to obtain a reliable data comparison. Two periods were investigated: three summer days,
 387 1/08-3/08, and three winter days, 1/01-3/01.
 388 The results demonstrated that the adoption of the reflective coatings on the building roof mainly
 389 impacts the zone air temperature of the beneath rooms, while negligible effects are obtained for
 390 the areas located two or more levels beneath. The traditional coating leads to the highest indoor
 391 air temperature due to its high absorptance, while the reflective roofs provide significant indoor
 392 air temperature reduction, especially in the summer period.

393 When the upper floor was considered, thermochromic paints applied on walls decreased the
394 indoor air temperature of almost 0.8 °C during winter, while during three summer days, the value
395 was more than doubled, being 1.75°C. The low U-value of the building leads to a more relevant
396 impact on the indoor air temperature. The adoption of reflective paint on the roof, instead,
397 induces a decrease of the room temperature, but the effect is less pronounced: an average
398 reduction of 0.5 °C and 0.3 °C was obtained for the cool and thermochromic coatings during the
399 winter analysis period, while a 1.3 °C and 1.6 °C reduction was obtained during the summer
400 period respectively.

401 The indoor temperatures differences are a consequence of the different amounts of heat transfer
402 through the building envelope, which are directly linked to the exterior surface temperature and
403 their respective variations. Two comparisons have been performed: thermochromic walls have
404 been compared to conventional high absorbing walls, while a conventional (dark) roof has been
405 compared to a cool and a thermochromic one. An HVAC system has also been introduced to
406 stabilize the indoor temperatures between 18 °C and 26 °C using different schedules. Figure 6
407 illustrates the exterior surface temperature trends and their relation to outdoor air temperature
408 and incident solar radiation, comparing the effects obtained by thermochromic paint and
409 conventional paint during the three hottest days of summer.

410 Each façade temperature trend shows a peak during a different period of the day accordingly to
411 the orientation; as expected, the peak for the east-facing wall occurs during the early hours of the
412 day (9:00-10:00 am), while the west-oriented one during the afternoon (5:00-6:00 pm), and no
413 clear peaks is measured for the north-facing surface.

414 The increased reflectance of the wall, due to the application of the thermochromic paint, has
415 decreased the peak temperature otherwise reached using conventional coatings. Excluding the
416 north wall, for the other three surfaces, an overall temperature reduction is achieved throughout
417 the whole day. In particular, during the hottest day (1/08), the south façade peak temperature has
418 shifted from 45.9 °C to 31.9 °C at 2:00 pm, for the east one from 44.5 °C to 30.5 °C at 9:30 am.
419 The south-west oriented wall is the one where the higher benefit is achieved: the difference
420 between the thermochromic and the conventional high absorbing wall simulations has reached a
421 maximum of approximately 23 °C (from 54.5 °C to 31.0 °C) at 5:30 pm.

422 Solar radiation plays a key role since the outdoor temperature is not particularly elevated. During
423 the last day displayed in the graphs, the weak direct solar radiation and low diffuse solar
424 radiation, probably caused by a clouded sky, leads to a very limited surface temperatures
425 difference between the two scenarios since the thermochromic transformation does not occur
426 (Fig. 6).

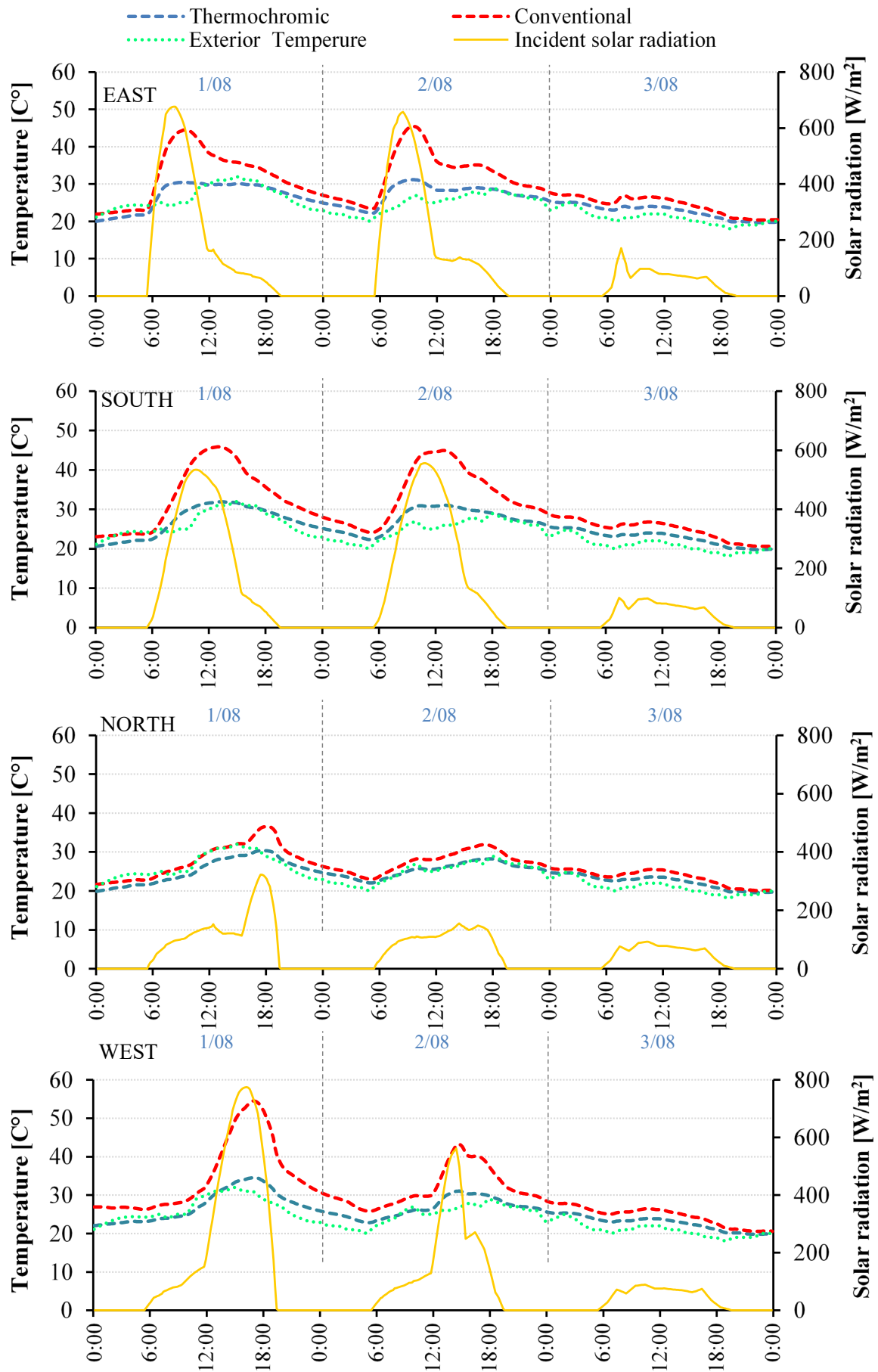
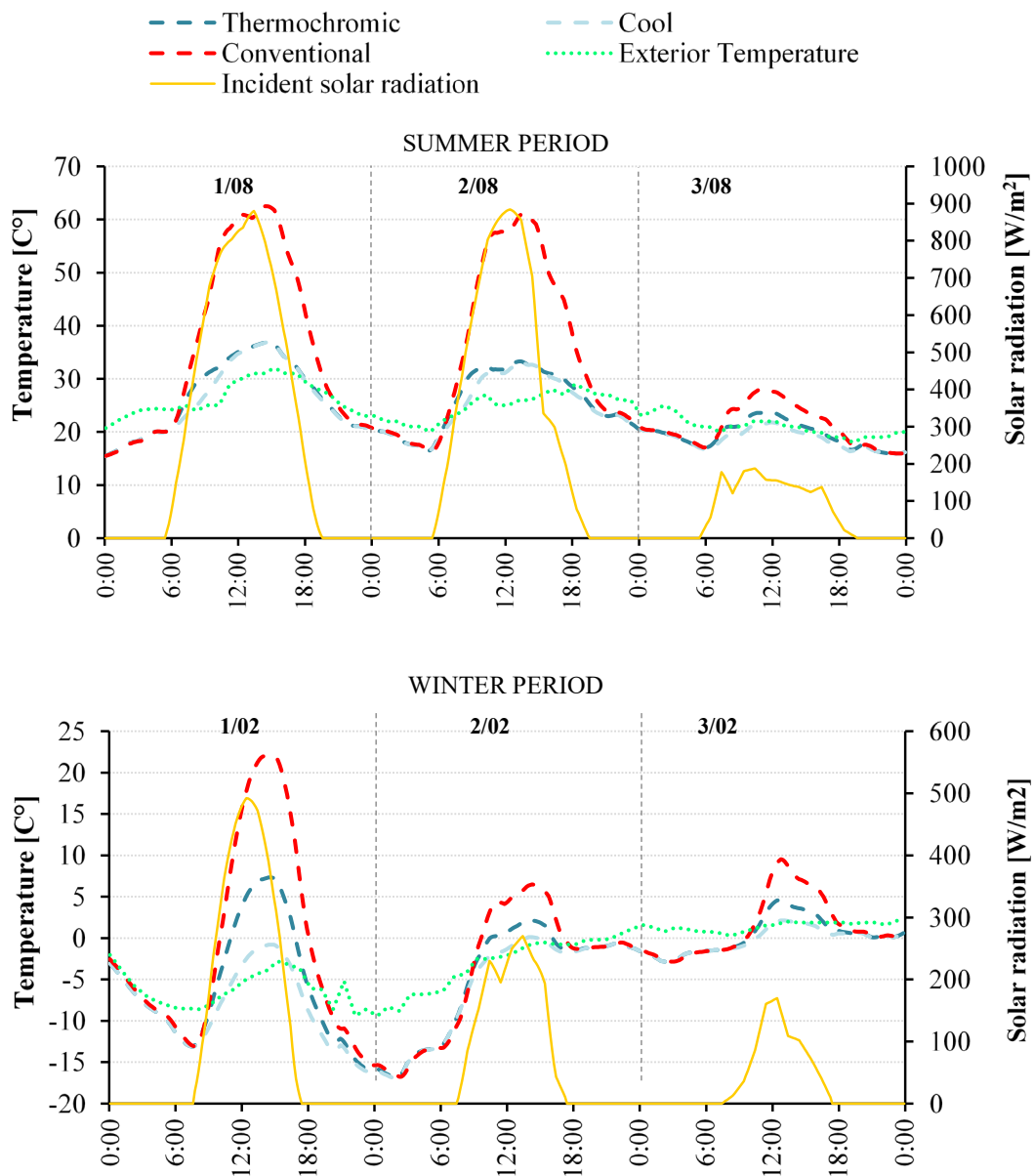


Figure 6. Wall surface temperatures comparison during three summer days (1st-3rd August).

429 The benefits achieved are even more significant on the roof since it is the surface that receives
 430 the most considerable amount of solar radiation. Both thermochromic and cool material achieved
 431 a significant surface temperature reduction: the peak is reduced from 62.5 °C to 37 °C.
 432 Thermochromic and cool paint achieve similar results since the solar reflectivity of the two
 433 solutions are similar. Small differences are observed during the early hours of the day when the
 434 thermochromic transformation has not occurred yet. The thermochromic paint completely shifts
 435 to the colorless phase after the solar radiation heats the surface for approximately one hour,
 436 between 6:00 and 7:00 am. During the 3rd of August, the drastic decrease of the direct radiation
 437 incident, coupled with relatively warm air temperature (max 20 °C), caused the surface to be not
 438 hot enough so that the thermochromic transformation could occur (Fig. 7).



439
 440 **Figure 7.** Roof surface temperatures comparison during three summer (1st-3rd August) and winter days
 441 (1st-3rd February).

442 The opposite trend has been observed during three typical winter days: as expected, cool and
 443 thermochromic surfaces lead to lower surface temperatures; however, the differences are less
 444 pronounced compared to the summer days, especially during the coldest day when the outdoor
 445 temperature is the main factor influencing the surface temperature.

446 The annual energy consumptions highlighted some limits of the simulated reflective paints.
 447 Since the climate of Toronto is heating dominated, the high solar reflectance of the
 448 thermochromic during its colored phase reduces the benefits obtained during the cooling period,
 449 where the incoming solar radiation is partially reflected. Cooling days are considerably lower
 450 compared to the ones where the heating system is working; moreover, since the outside
 451 temperatures are not particularly elevated even during summer, a limited amount of energy is
 452 requested to cool down the building (Table 8).

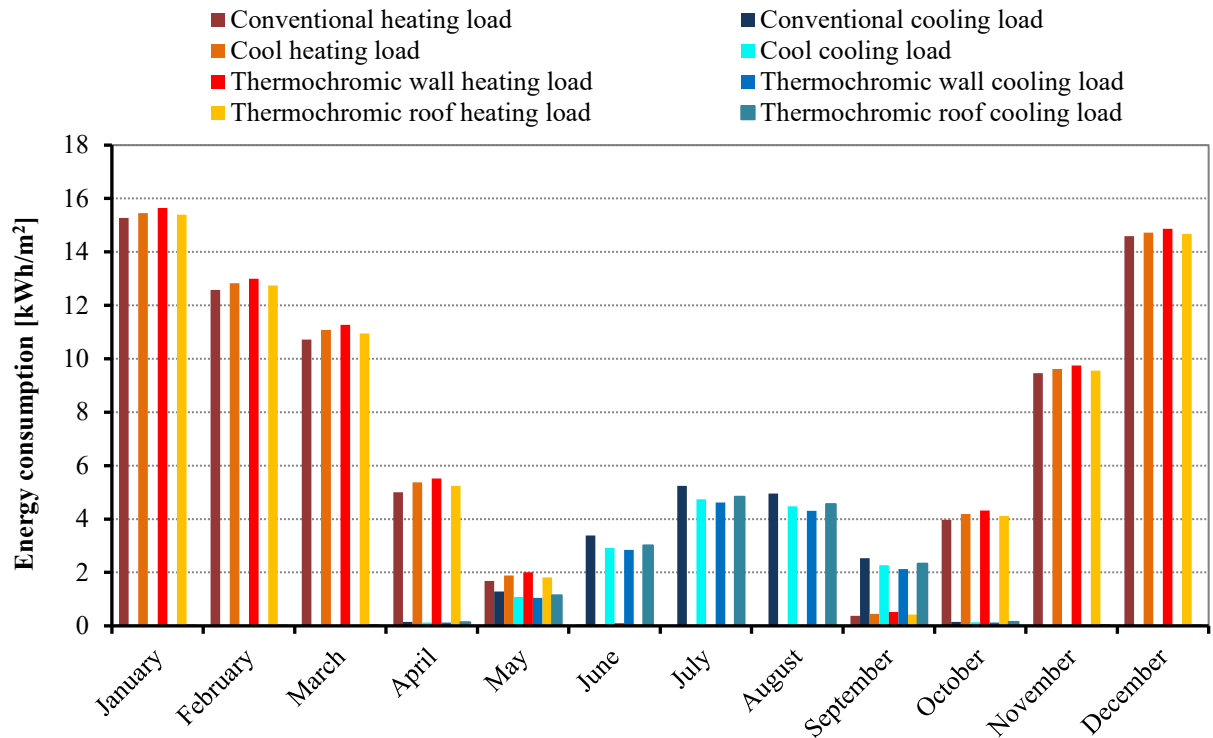
453

454

Table 6. Cooling benefits and heating penalties of the four different scenarios.

	EUI for conventional roofing [kWh/m ²]	Δ Cool roof	Δ TCM roof	Δ TCM wall
Cooling Load	17.8	-11.0%	-8.9%	-14.2%
Heating Load	73.7	+2.6%	+1.7%	+4.4%
Total	91.5	0%	-0.4%	+0.8%

455



456

457 **Figure 8.** Monthly energy consumption comparison: conventional, cool roof, thermochromic wall,
 458 thermochromic roof.

459 Even if the overall energy consumptions are not significantly reduced, it is clear that, for this
460 specific building, the adoption of a thermochromic roof is preferable compared to a cool or a
461 conventional roof. The higher absorptance of the thermochromic paint contained the heating
462 penalties to 1.7% during the cold season, while the thermochromic transformation allows a 9%
463 reduction of the cooling energy demand during the summer months. Cool roofs are less efficient
464 compared to the previous solution as a consequence of their static behavior, even though the
465 cooling savings are higher (-11%), the higher heating demand (+2.6%) nullifies the benefits.
466 Thermochromic walls are not a suitable alternative to conventional paint. Since the heating
467 consumptions are responsible for almost 80% of the total energy demand, the reduction of the
468 potential solar heat gain caused by the higher reflectance of thermochromic paints compared to
469 conventional high absorbing coatings has led to relevant heating penalties during the winter
470 season (+4.4%). The heating penalties are larger compared to the scenario where thermochromic
471 paint is applied on the roof since façades cover a larger portion of the building envelope;
472 therefore, a higher amount of radiation is reflected, and less heat is transfer into the building.

473

474 **4.2.2 Parametric analysis**

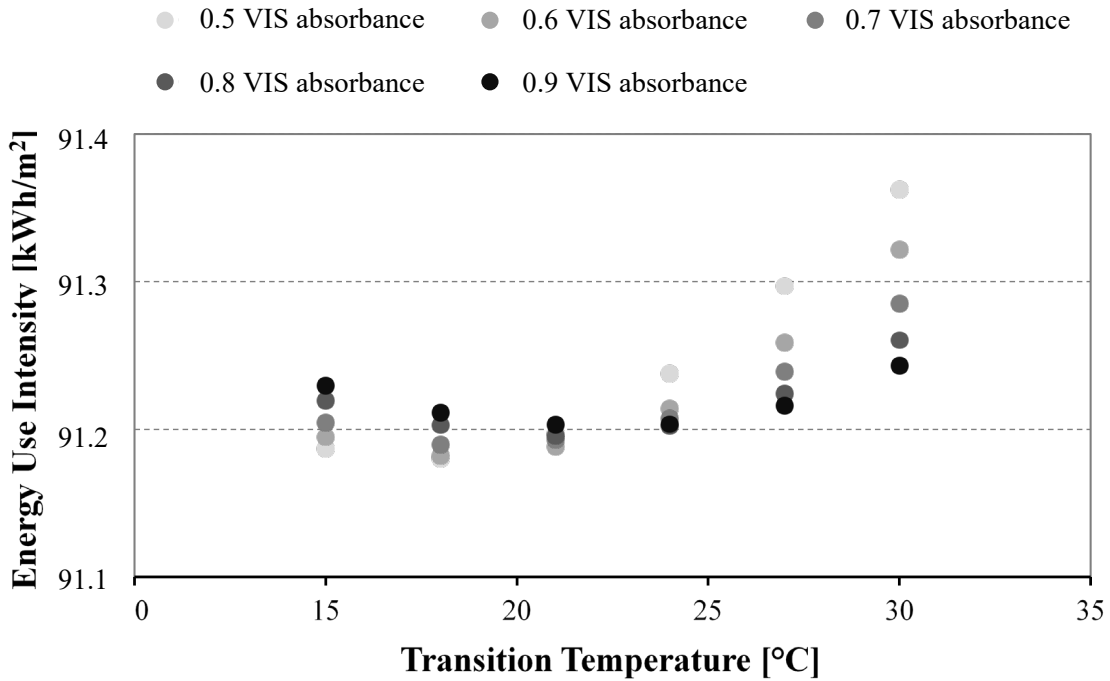
475 The results show that the thermochromic paint with the lowest solar absorptance, 0.5, and a
476 temperature transition of 18°C is the preferable solution. This solution maximizes the cooling
477 benefits, thanks to the high solar reflectance and the low transition temperature, which allows the
478 paint to reach its colorless phase more frequently.

- 479 • Colored: Visible absorptance = 0.5
- 480 • Colorless: Visible absorptance = $0.5 - 0.2 = 0.3$

481 Figure 9 illustrates how the best-case scenario slowly shifts from maximizing the cooling
482 benefits when the reflectivity is higher, to the reduction of the heating penalties as the solar
483 absorptance increases. A turning point is observed around the 21°C transition temperature. For
484 high transition temperature, a low reflective paint is preferable: since the thermochromic
485 transformation rarely occurs, a higher absorptance guarantees the limitation of heating penalties.
486 A higher reflectivity is suitable when the transition temperature is lower since the thermochromic
487 transition comes into play more frequently. While the solar absorptance has a more significant
488 impact on the energy consumption above the turning point, below the 21°C, the differences are
489 less significant since the heating demand has a more substantial effect on the overall energy
490 consumptions. However, the improvements obtained by changing the transition and solar
491 absorption are not substantial; the difference between the worst and best-case scenarios is less

492 than 1%. The relatively low improvement is a consequence of the negligible effect of the
 493 thermochromic paint achieved on the lowest floors of the building.

494

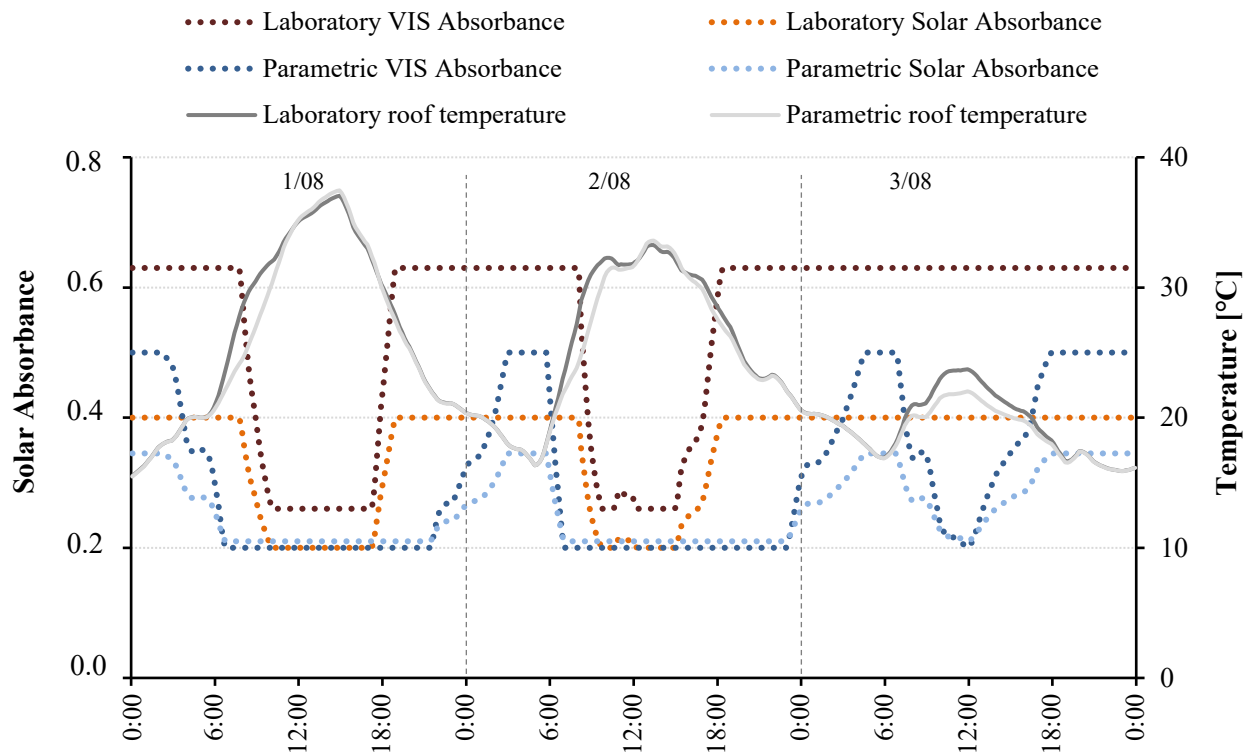


495

496 **Figure 9.** Parametric analysis results: annual energy use intensity comparison resulting from the different
 497 combinations of transition temperature and visible absorbance.

498

499 The best performing scenario of the parametric analysis ($T_{trans} = 18^{\circ}\text{C}$; solar absorptance_{colored} =
 500 0.35; solar absorptance_{colorless} = 0.21) has been compared to the lab paint created including the
 501 Black LT-31BF Kelly powder with a 15% concentration in the mixture ($T_{trans} = 28^{\circ}\text{C}$; solar
 502 absorptance_{colored} = 0.40; solar absorptance_{colorless} = 0.20). The solar reflectance of the two
 503 simulated paints is similar during both phases, even if the lab paint is slightly more absorptive
 504 when colored. The main difference is the transition temperature at which occurs the
 505 thermochromic transformation. Therefore, the main variation registered between the two
 506 scenarios is that the thermochromic transformation occurs more frequently and earlier compare
 507 to the other scenario, as illustrated in Fig.10. The transformation begins approximately five hours
 508 before the thermochromic lab paint. Consequently, the registered roof surface temperatures are
 509 lower until the thermochromic lab paint reaches its colorless stage; even the peak temperature
 510 has been reduced by 0.5 °C. It is interesting to notice that the thermochromic transformation also
 511 occurs on the third day when the outdoor temperature and the amount of incident solar radiation
 512 is lower compared to the previous days. However, since the thermo-optical differences are
 513 limited, the total energy use intensity has not changed.



514
 515 **Figure 10.** Roof surface temperature trends and thermo-optical properties: laboratory paint and best-case
 516 scenario of the parametric analysis during three summer days (1/08-3/08).

517
 518 **4.2.3 Context analysis**

519 The solar radiation and shadows studies performed with Ladybug proved that the most affected
 520 areas are the north and the east oriented facades; a partial decrease of the radiation has also been
 521 registered on the east side of the roof and in the lowest zone of the south and west façades. The
 522 incident radiation on the east facade is reduced by approximately 500 kWh/m² throughout the
 523 entire year. Regarding the Energy Plus simulations, the focus has been pointed mainly on the
 524 east façade, where the most relevant variations of the thermochromic transformation could be
 525 registered.

526 The results reported a substantial reduction of the incident radiation, which has led to a
 527 significant decrease in the surface temperature. Previously, the maximum temperature reached
 528 by a facade covered with a conventional paint was approximately 45 °C, the introduction of
 529 shading elements has reduced the peak temperature of almost 15 °C. As a consequence, the
 530 application of thermochromic has been less effective, and the achieved temperature reduction has
 531 been less than 5 °C.

532 Table 9 summarizes the impact of the context on four surfaces having different orientations;
 533 more precisely, it describes the amount of time during which the thermochromic transformation

534 occurs. The context has an impact also on the roof; however, only a small portion is affected, and
 535 the effect is less relevant compared to the shading on the walls.

536 **Table 7.** Influence of the context on the thermochromic transformation.

		East	South	North	West	roof
Context	N° hours max R%	0	0	0	4	92
	% over the total period	0	0	0	0.05	1.05
	N° hours intermediate R%	13	343	10	298	711
	% over the total period	0.15	3.90	0.10	3.40	8.10
No Context	N° hours max R%	0	0	0	6	93
	% over the total period	0	0	0	0.07	1.05
	N° hours intermediate R%	212	378	30	353	721
	% over the total period	2.40	4.30	0.35	4.05	8.20

537
 538 The context introduction increased the heating consumption by 9%, while the cooling demand
 539 has been reduced by 33% in the common case scenario, as a consequence of the less radiation
 540 incident on the building envelope. The surrounding buildings offer a significant shading effect
 541 both on the wall and on the numerous windows characterized by a low U-value. It is interesting
 542 to notice that when the context is included, all the proposed reflective technologies are
 543 counterproductive: the adoption of reflective paint leads to an increase of the energy
 544 consumptions ranging from of 1.1% when the thermochromics are applied on the facade, to a
 545 0.2% in the best case scenario when the thermochromics are used on the roof.

546

547 **Table 8.** Energy consumption comparison: context included.

	Conventional [kWh/m ²]	Cool roof	TCM roof	TCM wall
Cooling load	11.9	-12.5%	-10.1%	-12.3%
Heating load	80.3	+2.6%	+1.7%	+3.1%
Total	92.2	+0.6%	+0.2%	+1.1%

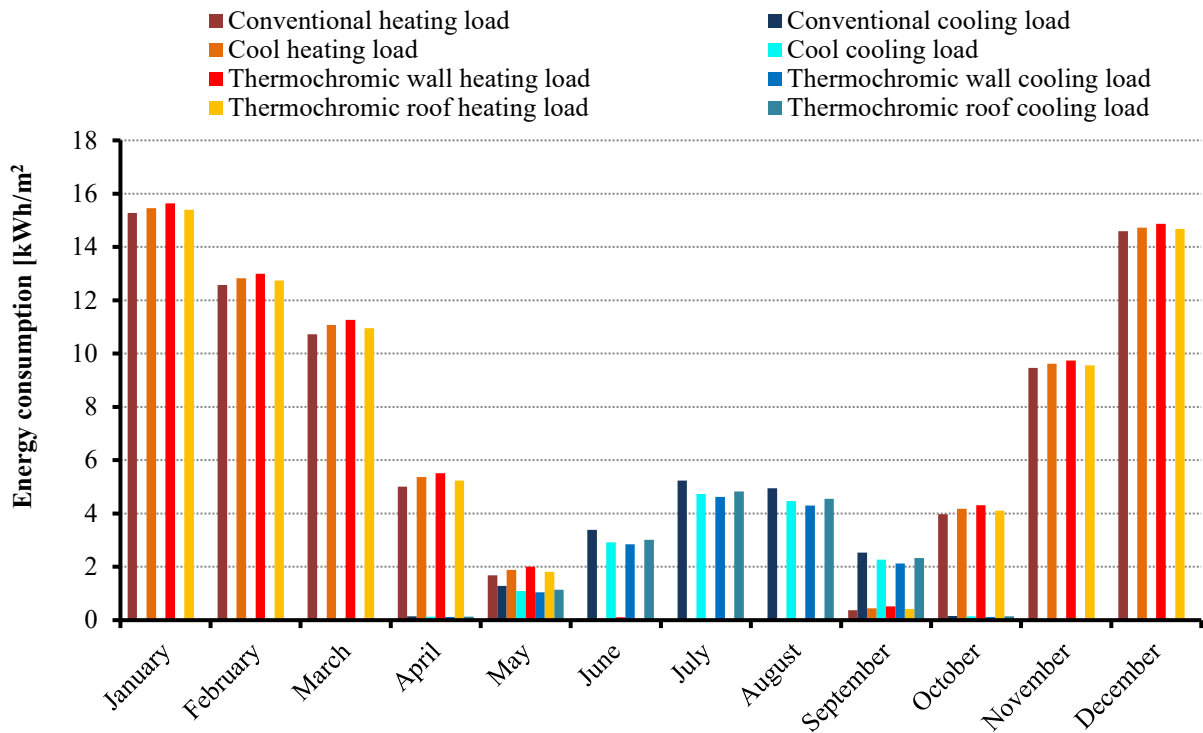
548

549 **4.2.4 Climate change impact**

550 The results highlighted a significant variation in the distribution of the energy demand of the
 551 building due to the mean temperature increase of 3.7–4.5 °C forecast by the future weather file.
 552 This increment has led to a doubling of the cooling consumption from 17.8 kWh/m² to 35.2 8
 553 kWh/m² while the heating demand reduced by 20% from 73.7 kWh/m² to 58.6 kWh/m². Besides,

554 the total energy use intensity increased by approximately 2.5%, from 91.5 kWh/m² to 93.8
 555 kWh/m².

556 Those changes have a significant impact on the effectiveness of reflective paints since their
 557 contributes become more relevant due to the increased necessity of reducing the cooling demand
 558 of the building, whose impact on the overall energy consumption has shifted from 20% to 38%.
 559 The cooling benefits achieved during the summer outweigh the heating penalties; thermochromic
 560 walls become the most effective solution guaranteeing a reduction of almost 11% of the cooling
 561 demand, leading to a reduction of the energy use intensity of 1.5%. Once again, thermochromic
 562 paints ensure lower energy consumptions compared to cool and conventional paints if applied on
 563 the roof: the cooling load is reduced by 6%, while the heating penalties are the lowest one 1.5%.
 564



565
 566 **Figure 11.** Monthly energy consumption comparison between four different scenarios: climate change
 567 impact.

568 **Table 9.** Energy consumption comparison: climate change impact.

	Conventional [kWh/m ²]	Cool roof	TCM roof	TCM wall
Cooling load	35.2	-7.0%	-6.1%	-10.7%
Heating load	58.8	+2.4%	+1.5%	+4.1%
Total	93.8	-1.2%	-1.3%	-1.5%

569 **5. Discussion**

570 The aim of this research was the investigation of the potential energy benefits resulting from the
571 application of thermochromic paints as a strategy to control solar loads. The experimental tests
572 highlighted the significant visible reflectance change occurring during the thermochromic
573 transformation: among the twelve different investigated paints, the maximum variation recorded
574 is 0.37, corresponding to a variation of the total solar reflectance of 0.20. Variations of the same
575 order have been obtained in previous studies (Fabiani et al., 2019; Zhang & Zhai, 2019). The
576 results testified the influence of the concentration of thermochromic particles on the total solar
577 reflectance: a higher amount of thermochromic pigments decrease the reflectivity of the paint. A
578 high solar reflectance characterizes the tested thermochromic paints in both phases due to the
579 high percentage of TiO₂ particles included in the basic paint mixture. As already reported by
580 Zhang & Zhai (2019) and Karlessi et al. (2009), TiO₂ particles are responsible for the increment
581 of the solar reflectance of thermochromic paints. The same trend observed for solar reflectivity
582 has been observed for the SRI values. However, the study results were limited by the basic
583 receipt used for the preparation of the prototype thermochromic paint: additives that prevent the
584 aging or improve the workability have not been introduced, and the purchased thermochromic
585 powders are products that have not been specifically designed for outdoor applications.

586 The second step of the study was the evaluation of the potential decrease of the energy
587 consumptions deriving from the adoption of thermochromic paints. Despite the reduction of the
588 cooling demand, 11% and 9% achieved by cool and thermochromic paint when applied on the
589 roof, the heating penalties deriving from the less heat absorbed during cold season balanced the
590 overall energy consumptions of the building, even if thermochromic proved to be more
591 performative confirming what has been observed by Jianying & Xiong (2019). The limited
592 overall energy savings could be explained considering two factors: the long and severe winter
593 climate in Toronto, and the peculiar characteristic of the case study building.

594 The situation was reversed when the future long-term changes in the outdoor climate conditions
595 are considered, due to the higher mean air temperature, the cooling load was increased, and the
596 heating one was reduced by 20%; as a consequence, reflective paints, in particular
597 thermochromic, guarantee a decrease of the total energy use intensity between 1.3% and 1.5%.
598 However, it must be specified that only one of the possible future scenarios has been simulated.

599 Contrary to previous studies, where only a single zone or small buildings were analyzed, the
600 simulated case study had four levels, and its roof was sufficiently insulated (U-value = 0.37
601 W/m²K). It is recognized that the effectiveness of reflective paints is limited to the zone just

602 below the roof, and the benefits are larger if the envelope is poorly insulated, as reported in a
603 recent research conducted by Zhang et al. (2020) on a two-story and less insulated office.
604 To have a complete overview of all the environmental parameters and context influences, a
605 factor that should be implemented and discussed in future studies, especially in cold climates, is
606 the snow accumulation on the roof. Hosseini & Akbari (2014) simulated the snow accumulation
607 considering the latter as an additional insulation layer characterized by specific solar reflectance
608 value (0.8-0.9 for fresh snow, 0.3-0.4 porous dirty snow); the results proved that heating
609 penalties for cool roofs are usually overestimated.

610

611 **6. Conclusions**

612 Thermochromic paints and cool paints, due to the high solar reflectance, proved to greatly reduce
613 the temperature of the surface where they are applied. Besides the less heat transfer into the
614 building, lower exterior temperatures are fundamental to prevent chemical degradation processes
615 and thermal fatigue, increasing the lifetime of the envelope. Thermochromic paints reduced the
616 roof peak temperature of approximately 25°C. On the facades, a decrease between 15°C -20°C
617 has been registered, depending on the orientation of the wall. Those differences were largely
618 reduced when the surrounding buildings have been introduced in the simulation domain,
619 especially for the vertical facades. The inter-building effect limited the benefits achieved by
620 thermochromic paints since the thermochromic transformation occurred less frequently. This
621 aspect, coupled with a heating-dominated climate like Toronto, made reflective paints a
622 counterproductive solution leading to an increment of the energy demand ranging from 0.2% to
623 1.1% when the thermochromic paint was applied on the roof and wall surfaces, respectively.
624 Energy Plus proved to simulate thermochromic paints accurately. Nevertheless, this latter strictly
625 related to the time step selected since the frequency of the update of the surface properties is
626 linked to this parameter. Moreover, no component is currently available inside the software
627 library itself, making the designing and setting process time-consuming. Future building energy
628 simulations investigating different building typologies and climate conditions, especially more
629 temperate zones, are also needed considering different climate change scenarios. At the same
630 time, future laboratory tests should be focused on the limited change of the thermo-optical
631 properties and the rapid aging of thermochromic coatings, as these issues limits a proper
632 experimental verification of the benefits achievable resulted from the simulation analysis
633 preventing thermochromic coatings from being a viable solution to cool products.

634

635 **Acknowledgments**

636 The first author wishes to thank the NSERC Discovery Grant and the Ontario MRIS – Early
637 Research Award programs for their contribution and financial support that made possible this
638 research.

639

640 **References**

641 ASTM E1980 (2011), Standard Practice for Calculating Solar Reflectance Index of Horizontal
642 and Low-Sloped Opaque Surfaces. West Conshohocken, PA, US.

643 ASTM E903 (2012), Standard Test Method for Solar Absorptance, Reflectance, and
644 Transmittance of Materials Using Integrating Spheres. West Conshohocken, PA, US.

645 ASTM E1933 (2014), Standard Practice for Measuring and Compensating for Emissivity Using
646 Infrared Imaging Radiometers. West Conshohocken, PA, US.

647 Ascione, F. (2017). Energy conservation and renewable technologies for buildings to face the
648 impact of the climate change and minimize the use of cooling. *Solar Energy*, 154, 34–100.

649 Berardi, U., & Jafarpur, P. (2020). Assessing the impact of climate change on building heating
650 and cooling energy demand in Canada. *Renewable and Sustainable Energy Reviews* 121,
651 109681.

652 Fabiani, C., Castaldo, V. L., & Pisello, A. L. (2020). Thermochromic materials for indoor
653 thermal comfort improvement: Finite difference modeling and validation in a real case-study
654 building. *Applied Energy* 262, 114-147.

655 Fabiani, C., Pisello, A. L., Bou-Zeid, E., Yang, J., & Cotana, F. (2019). Adaptive measures for
656 mitigating urban heat islands: The potential of thermochromic materials to control roofing
657 energy balance. *Applied Energy* 247, 155-170.

658 Garshasbi, S., & Santamouris, M. (2019). Using advanced thermochromic technologies in the
659 built environment: Recent development and potential to decrease the energy consumption
660 and fight urban overheating. *Solar Energy Materials and Solar Cells* 191, 21-32.

661 Haberl, J. S., & Cho, S. (2004). *Literature Review of Uncertainty of Analysis Methods*. Report to
662 the Texas Commission on Environmental Quality. Energy Systems Laboratory.

663 Hensen, J. L., & Lamberts, R. (2019). *Building Performance Simulation for Design and*
664 *Operation*. Routledge.

665 Hosseini, M., & Akbari, H. (2014). Heating energy penalties of cool roofs: the effect of snow
666 accumulation on roofs. *Advances in Building Energy Research* 8, 1-13.

667 IEA. (2019). *Global Energy & CO₂ Status Report*. Retrieved from IEA:
668 <https://www.iea.org/geco/emissions/>

669 Jianying, H., & Xiong, B. Y. (2019). Adaptive thermochromic roof system: Assessment of
670 performance under different climates. *Energy & Buildings* 192, 1-14.

671 Karlessi, T., & Santamouris, M. (2013). Improving the performance of thermochromic coatings
672 with the use of UV and optical filters tested under accelerated aging conditions.
673 *International Journal of Low-Carbon Technologies* 10, 45-61.

674 Karlessi, T., & Santamouris, M. (2013). Research on Thermochromic and PCM Doped Infrared
675 Reflective Coatings. In D. Kolokotsa, M. Santamouris, & H. Akbari, *Advances in the*
676 *Development of Cool Materials for the Built Environment* (pp. 83-103).

677 Karlessi, T., Santamouris, M., Apostolakis, K., Synnefa, A., & Livad, I. (2009). Development
678 and testing of thermochromic coatings for buildings and urban structures. *Solar Energy* 83,
679 538-551.

680 Jandaghian, Z., & Berardi, U. (2020). Analysis of the cooling effects of higher albedo surfaces
681 during heat waves coupling the Weather Research and Forecasting model with Building
682 Energy Models, *Energy and Buildings* 207, 109627.

683 Markets, M. (2019). *Thermochromic Materials Market by Material, End-use industry, Region-*
684 *Global Forecast to 2024*. Retrieved from [https://www.marketsandmarkets.com/Market-](https://www.marketsandmarkets.com/Market-Reports/thermochromic-material-market-253699772.html)
685 [Reports/thermochromic-material-market-253699772.html](https://www.marketsandmarkets.com/Market-Reports/thermochromic-material-market-253699772.html)

686 Morini E., Nicolini A., Castellani B., Rossi F., & Berardi, U. (2018) Effects of aging on retro-
687 reflective materials for building applications, *Energy and Buildings*, 179, 121-132.

688 *Paris Agreement*. (2016). Retrieved from:
689 https://ec.europa.eu/clima/policies/international/negotiations/paris_en

690 Park, B., & Krarti, M. (2016). Energy performance analysis of variable reflectivity envelope
691 systems for commercial buildings. *Energy and Buildings* 124, 88-98.

692 Pisello, A. L. (2017). State of the art on the development of cool coatings for buildings. *Solar*
693 *Energy* 144, 660-680.

694 Ritchie, H., & Roser, M. (2017, May). *CO₂ and Greenhouse Gas Emissions*. Retrieved from Our
695 World in Data: <https://ourworldindata.org/grapher/temperature-anomaly?time=1898>

696 Santamouris, M., Synnefa, A., & Karlessi, T. (2011). Using advanced cool materials in the urban
697 built environment to mitigate heat islands and improve thermal comfort conditions. *Solar*
698 *Energy* 85, 3085–3102.

699 Soudian, S., Berardi, U., & Laschuk, N. (2020). Development and thermal-optical
700 characterization of a cementitious plaster with phase change materials and thermochromic
701 paint. *Solar Energy* 205, 282-291.

702 Synnefa, A., & Santamouris, M. (2013). White or Light Colored Cool Roofing Materials. In D.
703 Kolokotsa, M. Santamouris, & H. Akbari, *Advances in the Development of Cool Materials*
704 *for the Built Environment* (pp. 33-71). Bentham Science Publishers.

705 Synnefa, A., Dandou, A., Santamouris, M., & Soulakellis, N. (2008). On the Use of Cool
706 Materials as a Heat Island Mitigation Strategy. *Journal of Applied Meteorology and*
707 *Climatology* 47, 2846-2856.

708 Synnefa, A., Santamouris, M., & Akbari, H. (2007). Estimating the effect of using cool coatings
709 on energy loads and thermal comfort in residential buildings in various climatic conditions.
710 *Energy and Buildings* 39, 1167–1174.

711 UN Environment and International Energy Agency. (2017). *Towards a zero-emission, efficient,*
712 *and resilient buildings and construction sector. Global Status Report 2017.* Retrieved from
713 https://www.worldgbc.org/sites/default/files/UNEP%20188_GABC_en%20%28web%29.pdf
714 f

715 Xiong, Y., & Jianying, H. (2019). Design and characterization of energy efficient roofing system
716 with innovative TiO₂ enhanced thermochromic films. *Construction and Building Materials*
717 223, 1053-1062.

718 Yuanyuan, C., Yujie, K., Chang, L., Zhang, C., Ning, W., Liangmiao, Z., . . . Yi, L. (2018).
719 Thermochromic VO₂ for Energy-Efficient Smart Windows. *Joule*, 1707-1746.

720 Zhang, Y., & Zhai, X. (2019). Preparation and testing of thermochromic coatings for buildings.
721 *Solar Energy* 191, 540-548.

722 Zhang, Y., Zhu, Y., Yang, J., & Zhai, X. (2020). Energy saving performance of thermochromic
723 coatings with different colors for buildings. *Energy and Buildings* 215, 109920.

724 Zheng, S., Yi, X., Shen, Q., & Yang, H. (2015). Preparation of thermochromic coatings and their
725 energy saving analysis. *Solar Energy* 112, 263-271.

726 Wang, Y., Berardi, U., & Akbari, H. (2016). Comparing the effects of urban heat island effect
727 mitigation strategies in the city of Toronto. *Energy and Buildings* 114, 2-19.